Publications of the Astronomical Society of the Pacific
108: 682–687, 1996 August

Low-Mass Stars in an Outer Field in NGC 6397[1]

JEREMY R. MOULD,[2] ALAN M. WATSON,[3] JOHN S. GALLAGHER III,[4] GILDA E. BALLESTER,[5] CHRISTOPHER J. BURROWS,[6] STEFANO CASERTANO,[7] JOHN T. CLARKE,[5] DAVID CRISP,[8] RICHARD E. GRIFFITHS,[7] J. JEFF HESTER,[9] JOHN G. HOESSEL,[4] JON A. HOLTZMAN,[3] PAUL A. SCOWEN,[9] KARL R. STAPELFELD,[8] JOHN T. TRAUGER,[8] AND JAMES A. WESTPHAL[10]

Received 1996 February 29; accepted 1996 May 31

ABSTRACT. We have imaged a field 10′ from the center of the globular cluster NGC 6397 in the visible and *I* bands with WFPC2 on the *HST*. At a level which is severely limited by counting statistics in the small area so far studied, this field is richer in dwarfs with $I>21.5$ than the 4.′6 radius parallel field discussed by Paresce and colleagues. This indicates that the dynamical process of mass segregation is occurring in the cluster.

1. INTRODUCTION

NGC 6397 is the closest globular cluster to the Sun in apparent distance modulus, located at a distance of about 2.2 kpc. It has low metallicity with [Fe/H]$=-1.9$ (Djorgovski 1994, Zinn 1985) and a low latitude ($b=-12°$) and a reddening $E_{B-V}=$ 0.18 mag. It is therefore ideal for studies of the Population II luminosity function (Mould 1996), and the most comprehensive such work to date is that of Drukier et al. (1993). These authors saw "some indication of mass segregation" between an 11′ field and others in the radius range (4′, 6.′5) for stars with $M<0.32\ M_\odot$.

Paresce et al. (1995) have observed the cluster with WFPC2 and clearly show a plateau in the mass function between approximately 0.25 and 0.15 $M_\odot$. They note that such a mass function can arise either primordially or as a result of dynamical evolution. King et al. (1995) have observed a central field in NGC 6397 and find a deficiency of low-mass stars. In this paper we study a field further from the cluster center to begin to quantify the effects of mass segregation.

2. OBSERVATION, REDUCTIONS, PHOTOMETRY, AND CALIBRATION

Exposures of length 3×1200 s in F555W and 3×1200 s in F814W were obtained on 1994 September 19. A field 10′ north of the cluster center was located on the apex of the pyramid at RA=17:40:41.5, Dec.=−53:30:25 (2000). Burrows (1995) and Trauger et al. (1994) describe the instrument in more detail. The images were reduced following Holtzman et al. (1995a) and Watson et al. (1994) and combined using a standard cosmic ray rejection algorithm.

A total of 700 stars were found in the combined images of the three WF chips. Aperture photometry was performed using a 0.″2 radius aperture in each case. Appropriate aperture corrections ranging from 0.15 to 0.2 mag in the three chips were made to reach the 0.″5 standard adopted by Holtzman et al. (1995b). This outer cluster field is not so crowded that point spread-function (PSF) fitting offers any gains in photometric precision. We saw no evidence that aperture corrections showed any field effects within individual chips, nor was there any evidence of nonlinearity for these long exposure times.

A *V–I* color–magnitude diagram (CMD) of NGC 6397 is shown in Fig. 1. The most striking feature of the CMD is the main sequence. Photometry is recorded in Table 1. The (*x*,*y*) coordinates refer to the chip number identified in the columns headed "C" in this table. Table 1 can be downloaded from the first author's home page at http://msowww.anu.edu.au

3. THE LUMINOSITY FUNCTION

Following Paresce et al. the main-sequence luminosity function was determined from a series of color profiles at half-magnitude intervals from I = 18.75 to I = 24.25. These are shown in Fig. 2. The main-sequence count was derived from the excess over the baseline in two or three color bins in these histograms and is recorded in column (2) of Table 2. The uncertainty from counting statistics is given in column

[1]Based on observations with the NASA/ESA *Hubble Space Telescope.*

[2]Mount Stromlo and Siding Spring Observatories, Institute of Advanced Studies, Australian National University, Private Bag, Weston Creek Post Office, ACT 2611, Australia
[3]Department of Astronomy, New Mexico State University, Box 30001, Department 4500, Las Cruces, New Mexico 88003-8001
[4]Department of Astronomy, University of Wisconsin at Madison, 475 N. Charter Street, Madison, Wisconsin 53706
[5]Department of Atmospheric and Oceanic Sciences, University of Michigan, 2455 Hayward, Ann Arbor, Michigan 48109
[6]Space Telescope Science Institute, 3700 San Martin Drive, Baltimore, Maryland 21218
[7]Department of Astronomy, Johns Hopkins University, 3400 N. Charles Street, Baltimore, Maryland 21218
[8]Jet Propulsion Laboratory, 4800 Oak Grove Drive, Mail Stop 179-225, Pasadena, California 91109
[9]Department of Physics and Astronomy, Arizona State University, Tyler Mall, Tempe, Arizona 85287
[10]Division of Geological and Planetary Sciences, California Institute of Technology, Pasadena, California 91125

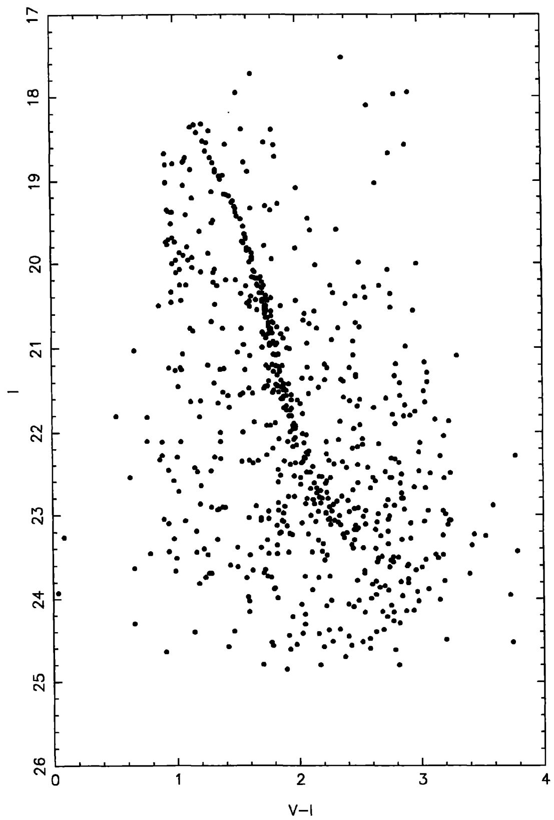

FIG. 1—Color–magnitude diagram for NGC 6397.

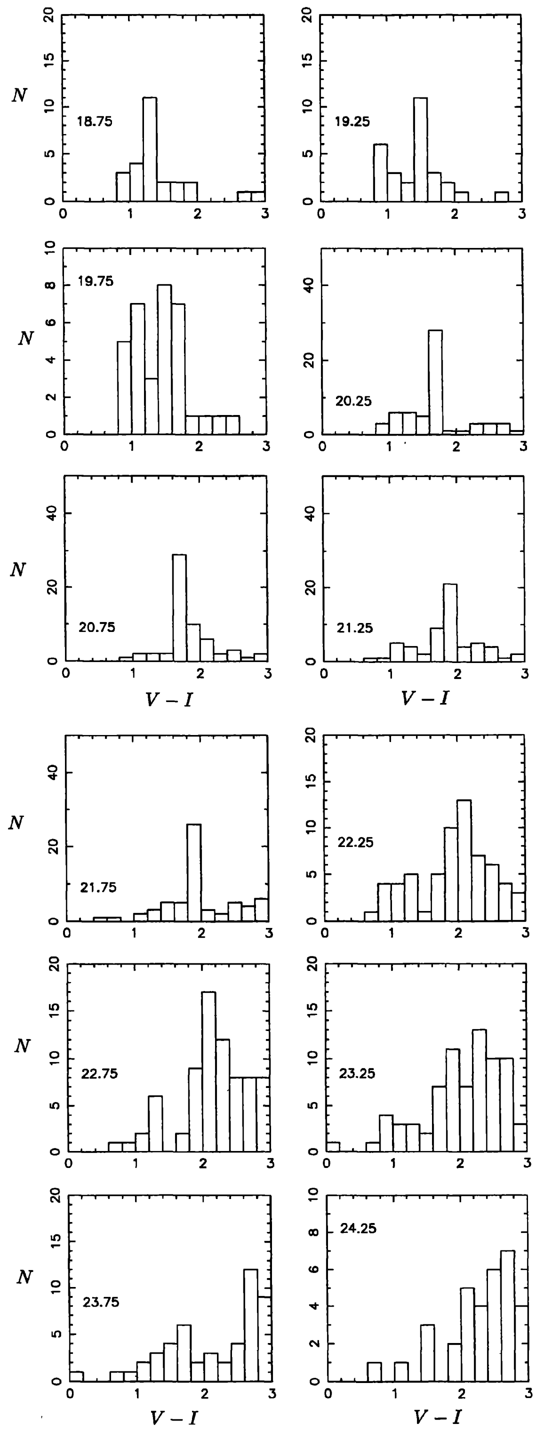

FIG. 2—Color distribution of stars at constant I magnitude. The I magnitude is shown on the left of each histogram.

(3) and is simply the square root of the corresponding entry in column (2). The uncertainty in the baseline is not the dominant error in this determination. The background correction is well determined for $I<23$ and small for $I<22$. The luminosity function determination was repeated with the color bins shifted by 0.1 mag without significant change in the result. We emphasize that small number statistics are the primary limitation of this determination. This can only be improved by observation of larger fields at this cluster radius.

Figure 3 shows that the number of bright main-sequence stars in 10′ field is close to expectations based on the 4.6′ field when scaled according to the star counts published by Da Costa (1982). For main-sequence stars fainter than $I=21.5$, we see an excess of stars in the 10′ field. The excess is 50% in these last four bins and is significant at a level exceeding 2σ.

To verify this we have recounted stars in the Paresce field using the original data from the *HST* archive. We used the same photometric techniques on the archive data as in our 10′ field. An even stronger effect is seen. Differences in Fig. 3 with the alternative 4.′6 luminosity functions are within counting statistics, however, for individual bins. These are dominated by the 10′ counts. If we collectively consider bins fainter than $I=21.5$, the faint star excess in the outer field over our recounted inner field is a factor of 2.5 and is both highly significant and significantly larger than the estimate from Paresce's luminosity function of a factor of 1.5. In the 4.′6 field background corrections are small for $I<23$ and therefore probably not the sole source of this discrepancy.

Paresce et al. note that the S/N of images brighter than $I=24$ is sufficiently high and the crowding in this field is sufficiently low that completeness corrections do not affect the luminosity function. To investigate this further, com-

TABLE 1
Photometry of NGC 6397

Star	$V-I$	I	C	x	y	Star	$V-I$	I	C	x	y	Star	$V-I$	I	C	x	y
1	2.20	22.13	3	627	67	49	2.79	21.39	3	622	196	97	2.11	23.10	3	742	308
2	2.20	22.61	3	119	69	50	1.91	21.04	3	209	197	98	0.96	19.42	3	772	311
3	2.37	24.46	3	675	76	51	2.42	21.96	3	563	197	99	1.48	19.37	3	620	312
4	1.80	21.24	3	234	81	52	1.82	22.11	3	409	198	100	2.57	22.55	3	225	314
5	1.35	18.98	3	577	87	53	1.69	21.03	3	690	199	101	1.77	21.23	3	369	314
6	2.33	23.24	3	42	90	54	3.47	23.16	3	613	200	102	1.88	21.76	3	565	314
7	1.49	17.99	3	485	93	55	2.54	24.60	3	389	204	103	1.81	20.79	3	353	315
8	1.71	20.55	3	218	95	56	2.53	22.43	3	670	204	104	1.28	18.76	3	426	316
9	2.45	22.92	3	393	100	57	1.88	21.71	3	445	213	105	1.75	20.98	3	508	316
10	1.80	18.74	3	745	109	58	1.83	23.24	3	632	214	106	3.14	23.73	3	56	317
11	1.78	20.74	3	556	110	59	1.89	20.81	3	768	218	107	1.84	20.87	3	351	317
12	1.74	21.27	3	457	114	60	1.84	20.54	3	288	224	108	3.11	22.24	3	159	321
13	2.22	23.07	3	740	114	61	2.45	22.62	3	95	226	109	0.97	19.42	3	454	321
14	0.94	19.41	3	543	117	62	2.71	24.06	3	97	229	110	1.72	20.68	3	297	322
15	1.86	21.53	3	121	120	63	2.19	23.00	3	93	236	111	1.13	19.97	3	529	322
16	2.34	17.53	3	230	125	64	1.55	23.78	3	207	237	112	1.89	21.03	3	307	330
17	2.44	21.32	3	700	126	65	1.81	21.35	3	352	242	113	1.81	21.47	3	52	334
18	1.04	21.29	3	546	128	66	1.99	24.09	3	268	244	114	1.73	20.68	3	167	335
19	1.92	24.24	3	197	130	67	2.29	19.60	3	696	244	115	1.60	20.43	3	557	338
20	2.42	23.18	3	133	131	68	1.63	20.21	3	360	248	116	1.79	21.92	3	672	338
21	1.69	20.39	3	77	134	69	2.94	22.21	3	160	250	117	1.21	18.36	3	338	343
22	2.12	22.70	3	752	134	70	1.13	20.09	3	331	252	118	2.67	22.88	3	106	344
23	1.86	22.38	3	472	138	71	2.98	21.47	3	511	258	119	2.54	24.48	3	605	351
24	1.92	21.58	3	397	139	72	1.70	20.47	3	41	259	120	2.61	23.50	3	524	353
25	1.72	22.31	3	72	141	73	2.22	22.36	3	306	259	121	1.86	21.50	3	750	353
26	2.32	21.38	3	564	146	74	0.97	20.04	3	292	262	122	2.47	19.99	3	92	355
27	2.19	22.64	3	736	153	75	1.75	23.77	3	680	262	123	2.84	18.54	3	421	365
28	1.90	21.45	3	428	156	76	1.84	21.63	3	763	263	124	1.32	18.90	3	227	373
29	2.09	22.44	3	158	162	77	2.06	21.56	3	240	267	125	1.03	20.30	3	312	376
30	1.78	20.96	3	694	162	78	2.58	21.70	3	400	267	126	1.90	21.83	3	301	378
31	2.03	22.34	3	182	167	79	2.17	23.36	3	510	269	127	0.86	20.54	3	424	379
32	2.55	22.68	3	513	167	80	1.45	24.43	3	347	270	128	1.64	20.47	3	441	382
33	1.73	23.08	3	591	173	81	1.84	21.49	3	717	272	129	2.70	20.06	3	350	389
34	1.80	21.12	3	457	174	82	2.91	23.62	3	403	275	130	2.49	23.39	3	433	391
35	2.06	19.48	3	170	175	83	2.89	24.11	3	535	275	131	1.58	22.38	3	139	392
36	2.84	20.96	3	363	175	84	2.59	23.39	3	208	276	132	1.06	19.09	3	447	392
37	1.52	19.50	3	707	175	85	1.33	20.31	3	505	279	133	2.73	23.48	3	246	396
38	1.06	19.94	3	72	180	86	1.81	20.98	3	458	282	134	2.05	23.25	3	391	399
39	1.67	23.42	3	394	184	87	1.60	19.37	3	206	285	135	2.80	22.72	3	238	401
40	2.99	21.60	3	310	186	88	1.31	20.53	3	436	288	136	2.16	22.56	3	412	401
41	2.73	24.14	3	187	187	89	2.19	21.39	3	68	289	137	4.75	22.09	3	426	402
42	2.36	20.49	3	590	190	90	2.47	21.61	3	317	289	138	2.02	22.15	3	118	414
43	1.60	23.69	3	608	190	91	2.72	22.30	3	71	290	139	1.38	18.97	3	595	420
44	1.07	18.80	3	215	192	92	1.92	21.64	3	223	295	140	2.13	20.79	3	345	425
45	2.04	22.83	3	434	192	93	1.30	18.82	3	79	303	141	2.45	22.18	3	494	428
46	1.89	23.47	3	441	192	94	2.23	23.13	3	323	304	142	2.51	20.29	3	318	429
47	2.73	23.54	3	169	193	95	1.65	20.29	3	445	305	143	2.74	24.60	3	794	434
48	2.75	21.88	3	458	193	96	2.18	23.55	3	42	306	144	0.92	18.84	3	166	436
145	1.56	19.72	3	632	436	193	1.53	18.42	3	291	641	241	2.41	22.20	3	338	797
146	2.15	22.73	3	398	441	194	1.17	18.46	3	533	641	1	2.59	23.17	2	471	37
147	1.89	24.47	3	106	445	195	1.10	20.00	3	643	655	2	1.69	20.26	2	490	41
148	1.88	21.53	3	190	451	196	1.54	21.00	3	451	656	3	1.96	20.47	2	177	42
149	1.77	18.42	3	176	455	197	3.36	23.28	3	39	657	4	2.85	23.56	2	625	42
150	2.19	21.21	3	125	456	198	2.87	17.92	3	194	658	5	2.24	22.97	2	687	43
151	2.90	22.64	3	45	458	199	2.16	23.45	3	693	661	6	2.34	21.59	2	284	48
152	0.62	22.58	3	687	463	200	1.72	20.54	3	783	672	7	1.70	21.51	2	424	48
153	3.19	22.44	3	285	468	201	3.03	22.46	3	438	676	8	0.86	22.37	2	697	50
154	1.59	20.49	3	387	469	202	1.42	21.74	3	628	676	9	1.57	19.85	2	373	59
155	2.08	19.62	3	370	475	203	1.95	24.58	3	560	678	10	2.16	22.82	2	303	61
156	2.59	23.78	3	504	481	204	1.61	22.41	3	80	679	11	1.81	21.48	2	463	62
157	1.73	21.48	3	397	482	205	1.08	19.45	3	597	690	12	1.71	20.63	2	75	63
158	1.12	18.40	3	412	483	206	1.92	21.83	3	791	692	13	2.23	22.57	2	766	63
159	2.32	22.79	3	248	485	207	2.81	22.78	3	258	695	14	2.55	23.99	2	734	67
160	2.17	24.60	3	206	487	208	1.30	21.45	3	622	696	15	0.04	23.93	2	675	74
161	1.63	22.93	3	138	488	209	1.27	22.95	3	117	699	16	1.35	22.36	2	197	80
162	1.00	20.00	3	405	490	210	1.78	21.11	3	380	700	17	1.41	21.60	2	422	80
163	2.83	21.65	3	616	497	211	2.07	20.74	3	761	706	18	1.26	19.92	2	771	81
164	1.53	21.57	3	699	505	212	2.07	23.03	3	637	711	19	1.62	21.91	2	258	92
165	2.22	23.74	3	206	510	213	1.57	24.06	3	76	718	20	1.69	23.72	2	212	95
166	1.68	20.20	3	287	513	214	3.07	23.42	3	132	721	21	1.73	22.99	2	440	97
167	1.56	20.31	3	332	523	215	0.96	19.56	3	362	723	22	1.58	18.92	2	96	102
168	1.37	21.56	3	169	525	216	1.69	20.85	3	515	730	23	1.22	18.56	2	724	107
169	1.11	20.81	3	286	531	217	1.72	20.42	3	559	730	24	0.93	23.47	2	642	112
170	3.38	23.15	3	728	537	218	2.11	20.59	3	707	732	25	2.44	21.34	2	656	112
171	2.63	23.24	3	567	540	219	2.31	21.88	3	152	733	26	0.88	22.32	2	636	118
172	1.94	21.92	3	365	543	220	2.60	23.55	3	306	735	27	2.20	22.28	2	234	120
173	2.77	23.48	3	392	549	221	1.80	23.39	3	485	735	28	2.45	22.40	2	744	122
174	1.67	23.10	3	623	552	222	1.52	20.81	3	51	742	29	2.47	20.76	2	563	124
175	1.72	23.33	3	173	556	223	1.92	23.26	3	136	745	30	1.86	22.93	2	556	131
176	1.81	22.89	3	117	563	224	1.76	19.39	3	590	747	31	1.30	20.15	2	65	131
177	1.03	21.27	3	636	565	225	2.50	23.69	3	205	748	32	2.05	21.25	2	381	134
178	1.25	21.24	3	43	567	226	1.65	20.22	3	717	749	33	0.99	23.55	2	574	134
179	2.21	22.82	3	303	573	227	2.85	23.78	3	776	750	34	0.93	22.50	2	620	134

TABLE 1
(Continued)

Star	$V-I$	I	C	x	y	Star	$V-I$	I	C	x	y	Star	$V-I$	I	C	x	y
180	1.77	22.23	3	556	579	228	2.77	24.78	3	464	753	35	0.89	23.09	2	616	137
181	1.96	22.18	3	503	580	229	2.82	22.91	3	268	754	36	2.48	24.52	2	328	138
182	1.55	21.29	3	643	581	230	2.80	22.78	3	431	757	37	1.92	21.74	2	469	138
183	1.57	20.51	3	205	599	231	2.39	21.63	3	422	763	38	0.65	23.66	2	613	140
184	2.72	20.35	3	602	599	232	1.71	21.49	3	298	769	39	1.67	20.39	2	361	141
185	2.07	22.51	3	343	602	233	3.34	23.62	3	235	771	40	1.52	22.39	2	120	143
186	1.38	22.95	3	512	602	234	2.22	22.92	3	54	776	41	1.61	21.57	2	171	144
187	2.19	22.99	3	241	613	235	2.04	22.05	3	273	777	42	2.36	23.22	2	345	145
188	2.47	21.91	3	569	628	236	1.84	21.41	3	278	778	43	2.80	22.49	2	185	147
189	1.32	22.98	3	683	629	237	1.33	22.97	3	109	783	44	1.27	22.51	2	457	153
190	2.69	23.33	3	325	632	238	1.97	21.64	3	89	788	45	1.30	22.34	2	486	154
191	1.06	23.11	3	544	634	239	2.69	22.81	3	444	789	46	1.22	23.78	2	555	153
192	1.77	21.56	3	559	636	240	3.71	22.17	3	78	790	47	2.79	22.60	2	188	161
48	3.15	24.44	2	102	163	96	1.72	23.76	2	179	330	144	1.13	19.25	2	363	487
49	1.99	22.66	2	636	165	97	2.09	22.84	2	193	339	145	1.90	24.64	2	284	505
50	2.38	22.97	2	179	166	98	2.31	23.13	2	571	339	146	1.15	23.48	2	297	508
51	0.92	19.78	2	265	166	99	1.72	20.45	2	80	350	147	1.80	24.02	2	163	511
52	2.51	23.11	2	620	167	100	1.86	20.92	2	105	352	148	3.01	23.84	2	265	524
53	1.71	19.82	2	733	167	101	2.36	22.44	2	437	354	149	2.14	21.48	2	224	525
54	2.21	21.25	2	768	167	102	1.83	22.56	2	669	354	150	2.70	23.00	2	341	529
55	1.45	19.30	2	317	171	103	2.21	24.39	2	476	356	151	0.92	19.05	2	368	530
56	2.60	23.08	2	416	175	104	0.96	20.50	2	590	357	152	2.25	20.92	2	794	531
57	3.17	23.06	2	367	176	105	0.76	21.85	2	66	358	153	1.75	21.01	2	765	533
58	1.68	24.83	2	642	179	106	1.62	20.12	2	157	361	154	1.57	19.88	2	704	535
59	0.94	19.75	2	463	181	107	3.01	21.36	2	603	366	155	1.30	20.27	2	175	543
60	1.18	21.85	2	459	184	108	1.90	23.25	2	133	374	156	1.77	20.86	2	692	549
61	1.42	23.63	2	302	187	109	1.95	22.40	2	260	375	157	1.74	20.78	2	576	551
62	1.72	20.58	2	248	189	110	0.98	18.83	2	420	375	158	1.73	20.48	2	656	561
63	2.91	21.72	2	120	191	111	1.80	21.46	2	118	379	159	3.66	23.84	2	315	564
64	1.32	18.93	2	520	191	112	1.82	23.25	2	128	379	160	1.78	21.31	2	568	566
65	1.59	20.55	2	329	193	113	2.01	22.04	2	169	385	161	2.79	23.77	2	583	566
66	2.40	23.36	2	343	195	114	1.95	21.96	2	429	385	162	2.14	22.81	2	198	569
67	0.97	19.73	2	269	196	115	1.48	23.42	2	121	386	163	1.57	23.07	2	95	574
68	1.95	21.94	2	554	196	116	1.76	20.66	2	181	386	164	1.61	19.99	2	546	584
69	1.85	21.63	2	598	204	117	2.41	22.71	2	524	387	165	1.72	20.60	2	450	586
70	3.15	22.94	2	269	207	118	2.82	21.78	2	570	389	166	1.71	20.54	2	660	586
71	2.62	22.13	2	244	211	119	2.33	22.37	2	769	392	167	1.30	19.52	2	212	589
72	1.41	19.21	2	797	214	120	0.66	21.06	2	71	394	168	1.83	21.29	2	517	590
73	1.93	21.99	2	214	215	121	1.29	19.55	2	228	400	169	1.59	19.87	2	793	592
74	2.80	23.94	2	539	215	122	1.01	22.76	2	104	403	170	1.27	23.73	2	728	594
75	2.73	21.77	2	603	216	123	2.37	22.84	2	117	415	171	2.34	21.40	2	188	595
76	1.64	20.22	2	667	232	124	1.82	21.11	2	362	417	172	3.01	21.25	2	85	603
77	2.44	20.71	2	105	238	125	2.71	18.65	2	200	419	173	2.42	20.93	2	767	603
78	3.01	22.91	2	372	239	126	2.79	21.54	2	387	419	174	1.61	20.20	2	204	604
79	3.53	22.79	2	122	240	127	1.27	18.44	2	346	436	175	1.95	22.09	2	371	604
80	2.02	20.70	2	413	245	128	3.19	23.01	2	456	438	176	1.08	20.30	2	246	606
81	2.68	21.58	2	588	259	129	2.13	23.32	2	709	439	177	2.70	23.60	2	265	607
82	1.46	19.28	2	334	260	130	4.57	24.83	2	84	441	178	2.34	24.71	2	350	609
83	2.45	24.02	2	207	262	131	2.96	23.58	2	174	444	179	1.53	22.03	2	214	613
84	2.04	22.27	2	314	263	132	2.24	20.28	2	110	446	180	1.88	21.59	2	318	613
85	1.74	20.76	2	460	269	133	2.50	24.16	2	406	450	181	1.66	20.31	2	468	614
86	1.16	22.52	2	290	272	134	2.75	21.31	2	129	455	182	2.15	22.88	2	485	620
87	1.70	20.88	2	524	274	135	2.59	24.39	2	390	463	183	1.74	20.87	2	664	621
88	1.71	20.57	2	236	277	136	2.78	22.35	2	576	470	184	1.76	20.99	2	480	628
89	2.64	23.48	2	223	279	137	1.48	23.65	2	241	471	185	2.02	24.21	2	545	644
90	1.46	19.28	2	510	292	138	2.00	23.12	2	370	473	186	2.82	21.78	2	170	655
91	2.03	20.62	2	520	292	139	3.13	22.90	2	251	476	187	1.12	18.90	2	490	655
92	1.69	20.49	2	232	293	140	1.86	21.45	2	708	480	188	2.75	22.31	2	61	656
93	1.85	23.11	2	502	301	141	2.22	23.06	2	338	483	189	3.09	23.46	2	265	665
94	1.61	19.91	2	164	314	142	1.69	20.47	2	645	483	190	2.56	23.82	2	775	668
95	0.51	21.83	2	294	314	143	1.32	23.33	2	748	484	191	1.75	24.56	2	697	670
192	2.20	22.75	2	384	672	19	1.76	20.60	4	484	103	67	1.70	23.68	4	667	250
193	2.01	21.38	2	254	673	20	2.68	24.20	4	604	106	68	1.35	22.15	4	372	251
194	2.25	22.89	2	136	689	21	0.91	18.71	4	154	109	69	2.59	23.94	4	254	257
195	2.44	20.40	2	152	689	22	1.84	23.10	4	148	114	70	2.30	24.38	4	234	261
196	2.65	24.36	2	794	692	23	2.99	22.64	4	357	114	71	1.19	22.69	4	782	263
197	1.19	21.66	2	434	694	24	2.99	23.49	4	251	115	72	0.99	21.30	4	136	266
198	0.65	24.33	2	692	696	25	2.06	22.25	4	58	118	73	2.63	20.26	4	575	271
199	1.78	20.97	2	246	700	26	2.71	22.54	4	171	118	74	1.95	21.98	4	504	276
200	2.13	24.44	2	580	703	27	0.93	19.81	4	238	121	75	1.97	19.11	4	64	277
201	1.56	24.01	2	453	714	28	2.07	22.71	4	264	123	76	1.52	20.40	4	578	279
202	0.76	22.14	2	467	715	29	1.54	19.79	4	734	125	77	1.72	20.92	4	408	282
203	1.94	22.81	2	756	720	30	2.29	23.10	4	601	127	78	1.15	18.37	4	163	283
204	2.76	21.17	2	785	724	31	1.59	20.02	4	404	128	79	3.72	23.31	4	433	285
205	2.85	23.73	2	202	735	32	2.24	24.53	4	687	129	80	2.28	22.85	4	627	285
206	1.04	20.48	2	768	736	33	2.80	22.72	4	731	134	81	2.42	23.30	4	431	290
207	2.19	24.10	2	563	737	34	1.06	18.81	4	759	134	82	1.71	18.57	4	164	292
208	1.39	19.20	2	759	740	35	0.78	23.49	4	346	137	83	1.81	22.98	4	286	295
209	2.59	22.59	2	555	745	36	1.88	23.16	4	744	137	84	2.72	22.54	4	301	297
210	2.10	22.64	2	422	748	37	2.12	20.04	4	564	147	85	0.96	20.38	4	335	309
211	2.34	23.28	2	251	751	38	2.30	23.02	4	533	150	86	1.89	22.81	4	647	309
212	2.43	23.13	2	100	755	39	1.69	20.47	4	181	152	87	1.43	19.22	4	326	316

TABLE 1
(Continued)

Star	$V-I$	I	C	x	y	Star	$V-I$	I	C	x	y	Star	$V-I$	I	C	x	y
213	2.93	23.99	2	374	765	40	2.87	23.07	4	668	157	88	3.14	22.51	4	554	320
214	2.39	24.57	2	92	771	41	1.47	19.35	4	628	164	89	2.10	22.89	4	259	324
215	1.87	24.88	2	73	779	42	1.08	18.76	4	474	167	90	2.61	22.98	4	274	330
216	1.17	23.85	2	59	785	43	1.76	20.81	4	610	174	91	2.93	19.97	4	703	331
217	1.85	21.24	2	322	789	44	1.21	23.44	4	70	176	92	2.49	22.15	4	634	333
218	1.53	19.77	2	750	791	45	1.63	20.14	4	55	176	93	2.69	23.18	4	661	342
219	1.72	19.34	2	313	792	46	2.73	24.25	4	182	177	94	2.30	22.10	4	599	345
220	1.61	17.76	2	235	796	47	3.10	23.96	4	106	178	95	2.30	20.78	4	157	346
221	2.76	17.95	2	286	796	48	2.80	23.27	4	653	183	96	1.67	23.07	4	458	349
1	0.97	22.63	4	160	46	49	1.81	22.49	4	94	186	97	1.31	20.11	4	122	350
2	1.24	18.68	4	139	47	50	2.41	24.10	4	419	187	98	1.54	19.59	4	252	355
3	1.82	21.25	4	163	54	51	3.13	23.19	4	391	188	99	2.87	23.25	4	326	355
4	2.98	23.04	4	404	54	52	3.25	21.03	4	438	194	100	1.94	22.56	4	293	356
5	2.14	22.56	4	199	58	53	1.78	23.90	4	100	202	101	2.92	23.88	4	596	358
6	1.99	22.58	4	737	63	54	2.45	21.69	4	664	206	102	1.77	23.91	4	705	358
7	3.13	23.42	4	481	65	55	1.20	20.14	4	420	209	103	0.09	23.27	4	782	368
8	1.72	21.95	4	283	68	56	2.01	22.38	4	131	214	104	1.19	19.65	4	328	373
9	2.61	23.52	4	368	71	57	2.13	23.76	4	550	214	105	1.70	20.30	4	704	378
10	2.74	22.87	4	408	71	58	2.87	21.77	4	250	223	106	1.13	24.44	4	624	380
11	2.02	24.33	4	232	72	59	2.05	22.29	4	618	225	107	1.51	21.59	4	452	389
12	1.95	21.96	4	58	77	60	2.42	22.93	4	111	229	108	2.84	23.58	4	597	389
13	1.40	18.60	4	561	79	61	1.96	19.84	4	386	232	109	3.18	21.81	4	222	391
14	2.12	22.76	4	101	90	62	1.32	18.93	4	796	241	110	1.91	21.76	4	198	395
15	2.44	23.78	4	160	92	63	2.60	19.02	4	298	246	111	1.48	19.42	4	218	395
16	2.67	22.47	4	253	96	64	1.36	19.02	4	91	247	112	1.82	19.31	4	460	395
17	1.37	20.81	4	621	96	65	3.18	23.01	4	498	249	113	1.40	24.62	4	47	398
18	2.62	23.85	4	750	97	66	2.00	22.40	4	402	250	114	1.89	22.14	4	410	398
115	2.26	22.40	4	240	405	157	2.49	23.02	4	573	500	199	1.03	20.11	4	303	636
116	1.75	21.95	4	775	407	158	0.93	23.14	4	46	501	200	2.99	21.13	4	215	639
117	1.40	20.24	4	73	408	159	2.02	23.75	4	424	515	201	3.68	24.41	4	102	644
118	1.74	21.42	4	185	412	160	1.59	21.13	4	599	515	202	0.99	19.78	4	388	644
119	1.77	20.73	4	435	413	161	1.80	23.16	4	291	518	203	2.69	23.04	4	558	644
120	2.26	23.08	4	115	414	162	1.49	19.47	4	402	518	204	1.24	23.51	4	666	648
121	2.42	21.09	4	590	416	163	2.44	23.18	4	609	523	205	0.92	19.06	4	87	652
122	1.86	21.74	4	610	420	164	1.76	24.60	4	662	524	206	1.35	22.04	4	196	660
123	2.08	23.46	4	328	424	165	1.83	21.31	4	53	526	207	1.14	22.47	4	182	661
124	1.29	19.17	4	361	433	166	3.07	21.80	4	446	528	208	2.00	24.44	4	341	664
125	0.93	19.39	4	745	434	167	2.51	22.95	4	389	534	209	2.04	22.51	4	221	672
126	1.85	23.01	4	334	437	168	1.69	20.39	4	278	537	210	1.57	24.19	4	558	676
127	3.14	21.99	4	294	445	169	2.72	20.51	4	124	540	211	1.05	21.11	4	54	679
128	1.55	18.81	4	363	445	170	2.03	22.89	4	70	542	212	1.76	20.45	4	407	680
129	3.95	23.33	4	516	452	171	0.94	21.27	4	109	542	213	1.91	22.42	4	732	681
130	1.25	23.73	4	147	453	172	1.99	21.68	4	285	544	214	1.35	21.29	4	736	684
131	1.36	22.95	4	765	457	173	1.93	21.94	4	257	549	215	1.69	20.33	4	220	688
132	1.03	22.15	4	770	458	174	1.80	23.49	4	61	550	216	1.58	21.51	4	424	691
133	1.86	21.60	4	669	460	175	2.39	21.24	4	123	551	217	1.56	19.74	4	137	692
134	1.09	19.84	4	559	464	176	1.01	21.49	4	646	551	218	1.77	19.98	4	612	693
135	0.88	22.15	4	776	464	177	2.37	24.07	4	177	560	219	2.41	23.40	4	312	694
136	2.20	23.49	4	234	465	178	1.58	23.51	4	243	566	220	1.65	22.38	4	51	701
137	1.74	20.74	4	475	465	179	2.52	20.41	4	430	566	221	2.78	24.27	4	335	715
138	2.08	23.91	4	53	466	180	1.49	21.09	4	733	573	222	1.15	23.23	4	753	715
139	1.13	20.84	4	331	466	181	1.33	21.69	4	756	580	223	2.94	22.44	4	222	716
140	1.61	19.96	4	654	467	182	2.13	22.98	4	389	581	224	2.05	20.97	4	326	725
141	1.66	20.22	4	91	468	183	1.75	20.82	4	540	581	225	1.72	21.24	4	80	737
142	2.69	23.88	4	311	471	184	2.64	24.14	4	115	582	226	1.79	18.60	4	252	737
143	1.55	19.68	4	454	472	185	1.00	20.15	4	527	583	227	1.48	20.24	4	775	740
144	1.71	20.59	4	743	473	186	2.66	23.83	4	304	586	228	2.21	23.07	4	405	745
145	2.45	23.16	4	574	475	187	2.50	23.66	4	55	587	229	2.08	21.38	4	633	745
146	1.00	22.34	4	330	478	188	2.95	22.09	4	166	589	230	2.02	22.33	4	519	753
147	1.25	18.58	4	378	483	189	1.38	21.28	4	239	594	231	1.18	22.91	4	591	759
148	1.72	20.42	4	596	485	190	1.73	23.49	4	778	599	232	0.98	23.70	4	120	768
149	2.26	20.37	4	171	487	191	2.23	24.03	4	614	602	233	0.97	23.32	4	118	770
150	1.80	21.00	4	265	488	192	2.71	23.52	4	487	607	234	1.65	20.59	4	323	773
151	1.78	21.53	4	69	490	193	2.49	22.08	4	139	610	235	1.11	21.67	4	104	775
152	2.54	18.10	4	246	491	194	2.90	20.53	4	728	611	236	1.28	20.73	4	417	775
153	1.93	22.20	4	507	493	195	2.14	24.82	4	434	618	237	1.91	22.02	4	635	783
154	1.81	22.64	4	414	497	196	2.83	24.12	4	320	620	238	1.82	21.55	4	740	787
155	2.01	21.80	4	422	497	197	1.03	19.91	4	495	620						
156	0.90	24.68	4	324	498	198	1.94	22.11	4	672	621						

pleteness corrections were calculated in chips 2 and 3 using the DAOPHOT program ADDSTAR (Stetson 1987). We used the WFPC2 PSF employed by Ferrarese et al. (1996) in the H_0 Key Project. One hundred stars were added across the full magnitude range of Table 1 in four separate simulations on each chip. This amounts to 800 added stars and in each of the inner and outer fields. The results are shown in Fig. 4. They are similar in chips 2 and 3 and the process was not extended to chip 4. We conclude from this figure that the effects of differential incompleteness between the 4'.6 and 10' fields are not significant in determining the luminosity function ratio in the two fields.

We therefore attribute the trend toward an excess of low-mass stars in Fig. 3 to mass segregation in the cluster. The excess is approximately a factor of 2 in the range (21.5, 23) in I, although we have not succeeded in fully understanding differences in luminosity function estimates in this range between the present work and that of Paresce et al. Dynamical

TABLE 2
Luminosity Function

(1) I (mag)	(2) $n(10')$	(3) $\pm$	(4) $n(4'.6)$ (scaled)	(5) $\pm$	(6) $n(4'.6)$ (scaled) (recount)
18.75	7	3	8	1	*
19.25	6	2	10	1	13
19.75	10	3	13	1	14
20.25	27	5	22	2	23
20.75	26	5	25	2	22
21.25	18	4	19	2	16
21.75	26	5	13	1	11
22.25	11	3	10	1	6
22.75	12	3	8	1	4
23.25	10	3	6	1	2

models of the cluster predict an increase of a factor of approximately 1.7 between the turnoff mass and 0.12 $M_{\odot}$ (Drukier 1995), which corresponds to the magnitude range (16, 23) in I. The precise prediction depends upon details of the model such as tidal radius, age, mass, and the character of the gravitational potential. The present statistics allow us to do no more than detect the trend and identify its likely physical basis.

4. SUMMARY

In a 10′ radial field in NGC 6397 the lower main sequence can be traced down to I=23 mag. Beyond I=23.5 mag, statistics do not allow us to follow the main sequence, and a larger sample would be needed to set useful upper limits on the luminosity function. In this regard our results support those of Paresce et al. (1995) and differ from the low-mass dwarf-rich luminosity function of Fahlman et al. (1989). Evidence for mass segregation is seen in the ratio of the luminosity functions in the 10′ field and a 4′.6 radial field. Complete photometry of the cluster with WFPC2 would be useful in constraining detailed dynamical models of NGC 6397.

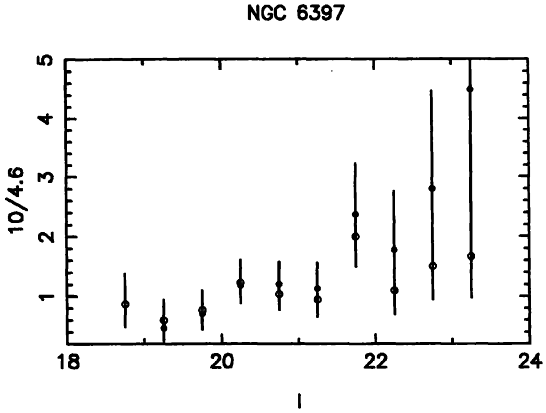

FIG. 3—The ratio of the luminosity functions in the 10′ and 4′.6 fields. The solid symbols are from column (4) and the open symbols from column (6) of Table 2.

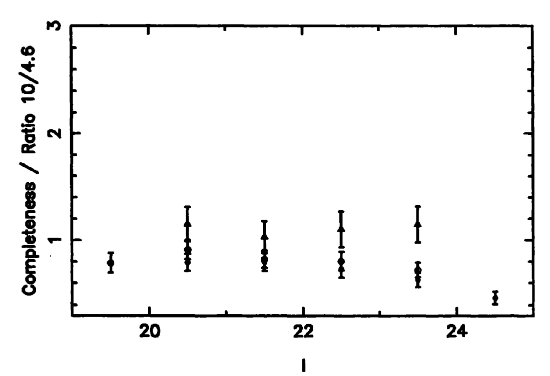

FIG. 4—Completeness in the 4′.6 field (solid symbols) and the 10′ field (open symbols). The expected ratio of star counts in the two fields as a result of completeness alone (i.e., in the absence of any mass segregation effects) is denoted by the triangles. The error bars are 1σ counting statistics.

This research was carried out by the WFPC2 Investigation Definition Team for JPL and was sponsored by NASA through Contract No. NAS7-1260. J.R.M. wishes to thank Gary Da Costa for helpful discussions and the referee for useful comments.

REFERENCES

Burrows, C. J. 1995, WFPC2 Instrument Handbook, 3rd ed. (Baltimore, STScI)
Da Costa, G. S. 1982, AJ, 87, 990
Djorgovski, S. G. 1994, ASP Conf. Ser., 50, 380
Drukier, G. 1995, ApJS, 100, 347
Drukier, G., Fahlmann, G., Richer, H., Searle, L., and Thompson, I. 1993, AJ, 106, 2335
Fahlmann, G., Richer, H., Searle, L., and Thompson, I. 1989, ApJ, 343, L49
Ferrarese, L., et al. 1996, ApJ (in press)
Holtzman, J. A., Burrows, C., Casertano, S., Watson, A., and Worthey, G. 1995b, PASP, 107, 1065
Holtzman, J. A., Hester, J. J., Casertano, S., Trauger, J., Watson, A., and WFPC2 IDT 1995a, PASP, 107, 156
King, I., Sosin, C., and Cool, A. 1995, ApJ, 452, L33
Mould, J. 1996, PASP, 108, 35
Paresce, F., De Marchi, G., and Romaniello, M. 1995, ApJ, 440, 216
Stetson, P. B. 1987, PASP, 99, 101
Trauger, J. T., et al. 1994, ApJ, 435, L3
Watson, A.M., et al. 1994, ApJ, 435, L55
Zinn, R. 1985, ApJ, 293, 424